IVP Analytic vs. Numerical Solution

July 13, 2020

1 Problem

To compare NOAA's Catalina 1, Nicolsky 2018 Analytic, and a finite volume method solutions of η in the following two shallow water problems:

1.1 A zero initial velocity N wave (Catalina 1)

$$\begin{aligned}\eta_0(x) = 0.006 * e^{-0.4444(x-4.129)^2} - 0.018e^{-4(x-1.6384)} \\ u_0(x) = 0 \\ h = x \\ m = \infty\end{aligned}$$

1.2 An N wave with initial velocity (Catalina 1 with initial velocity)

$$\begin{aligned}\eta_0(x) = 0.006 * e^{-0.4444(x-4.129)^2} - 0.018e^{-4(x-1.6384)} \\ u_0(x) = \eta_0(x)/\sqrt{x} \\ h = x \\ m = \infty\end{aligned}$$

In other words, a Gaussian initial wave with either no initial velocity or velocity defined as $u_0(x) = \eta_0(x)/\sqrt{x}$, and a plane-inclined bathymetry (y^∞). This reduces to a 1-1 SWE. We can reproduce this with a different slopes, different η_0, and different u_0.

2 Setup of the three Solutions

We are dealing with 3 solutions - NOAA, FVM, Nicolsky - and 2 Initial Conditions - zero velocity, non-zero velocity. 6 total scenarios. Of these 6, 5 were completed with the exception of NOAA non zero-velocity. NOAA zero velocity is still very rough.

All integrals were computed via Chebfun, a numerical computational tool designed to approximate functions with polynomials stably.

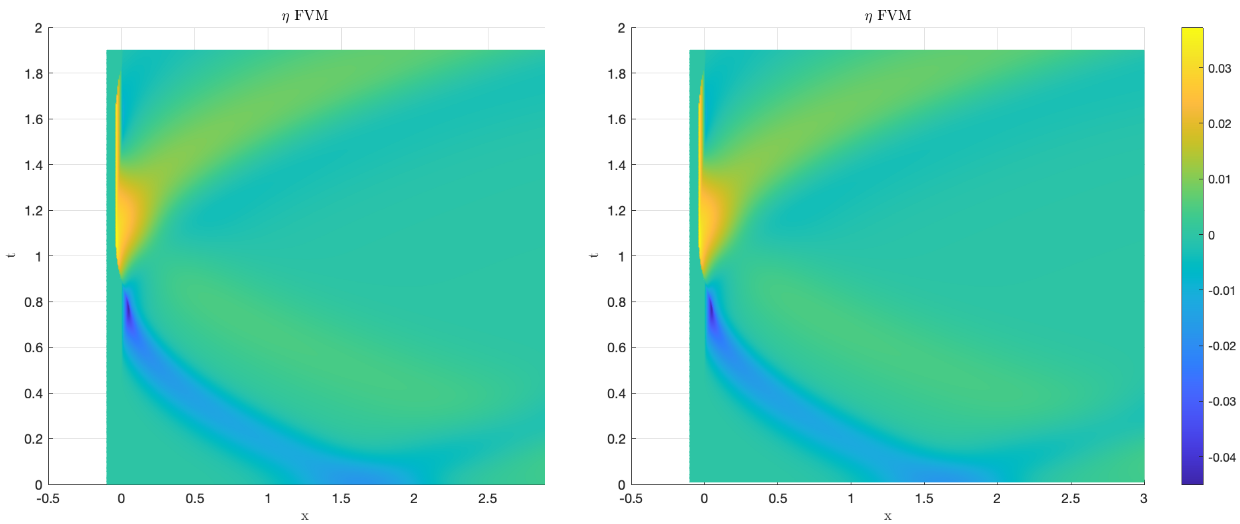

(a) Zero Velocity

(b) Non Zero Velocity

Figure 1: η FVM Solution over x:[-0.1 3] and t:[0 1.9]

2.1 Finite Volume Method

For the FVM we used Deny's Catalina 1 FVM. Initial conditions were set as height and flux where flux was computed by definition as hu where $h = \eta + x$. Both the zero velocity and nonzero velocity cases are depicted in Fig. 1.

2.2 Nicolsky 2018 Analytic

The analytical solution of η was computed using formulas in Nicolsky (2018). Please see Nicolsky 2018 for an extended explanation and derivation.

$$\psi(s,\lambda) = \int_0^\infty (a(k)cos(\beta k\lambda) + b(k)sin(\beta k\lambda))J_0(2k\sqrt{s})dk$$
$$\varphi(s,\lambda) = s^{-1/2}\int_0^\infty (a(k)sin(\beta k\lambda) + b(k)cos(\beta k\lambda))J_1(2k\sqrt{s})dk$$

where

$$a(k) = 2k\int_0^\infty \psi(s_*,0)J_0(2k\sqrt{s_*})ds_*$$
$$b(k) = 2k\int_0^\infty \varphi(s_*,0)s_*^{1/2}J_1(2k\sqrt{s_*})ds*$$

note that using change of variables $s_* = x_* + \eta_0(x_*)$ with a stipulation that $u_0 = 0$ then $a(k)$ and $b(k)$ can be transformed to

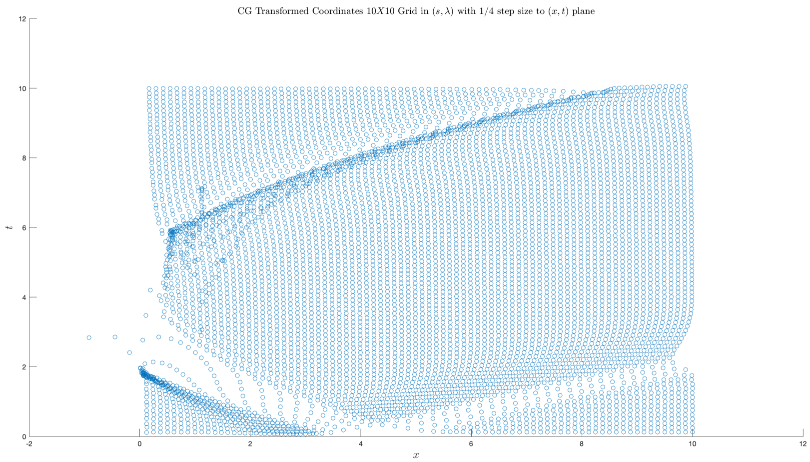

Figure 2: Note the distinct non-linear nature caused by the $-u^2$ of η

$$a(k) = 2k\int_{x_0}^{\infty} \eta_0(x_*) J_0(2k\sqrt{x_* + \eta_0(x_*)})(1+\eta_0'(x)ds*$$

$$b(k) = 0$$

This simplification was used in the zero velocity case in order to speed up computations. For the non-zero velocity case, the projection of φ and ψ onto $\lambda = 0$ were computed via a first order taylor expansion. Note that these equations require $\eta_0'(x) > -1$. See Nicolsky for explanation.

$$\Phi(s,\lambda) = \begin{pmatrix} \varphi(s,\lambda) \\ \psi(s,\lambda) \end{pmatrix}$$

$$\Phi_0(x) = \begin{pmatrix} u_0(x) \\ \eta_0(x) + u_0^2(x)/2 \end{pmatrix}$$

$$\Phi_1 = \Phi_0 + u_0(u_0' AD^{-1}B\Phi_0 - B\Phi_0 - AD^{-1}\Phi_0')$$

Chebfun was used to calculate the Hankel transform solution to the CG transform on a grid in (s,λ) then the nonlinear Carrier Creenspan transform to (x,t) Fig. 2 depicts this transform for a simple shifted Gaussian η_0. Figure 3 depicts the actual solution.

2.3 Catalina 1 NOAA

For this older analytic solution $\eta(\sigma,\lambda)$ and $u(\sigma,\lambda)$ are computed directly. However there is double integration in the computation of η and u unlike in the Nicolsky solution where single integration is used for the initial conditions and then for ϕ and ψ. Consequently, at least at this point, a highly accurate solution wasn't obtained.

$\eta_0(x)$ was transformed to $\Phi(\sigma)$ in Carrier Greenspan transformed space via

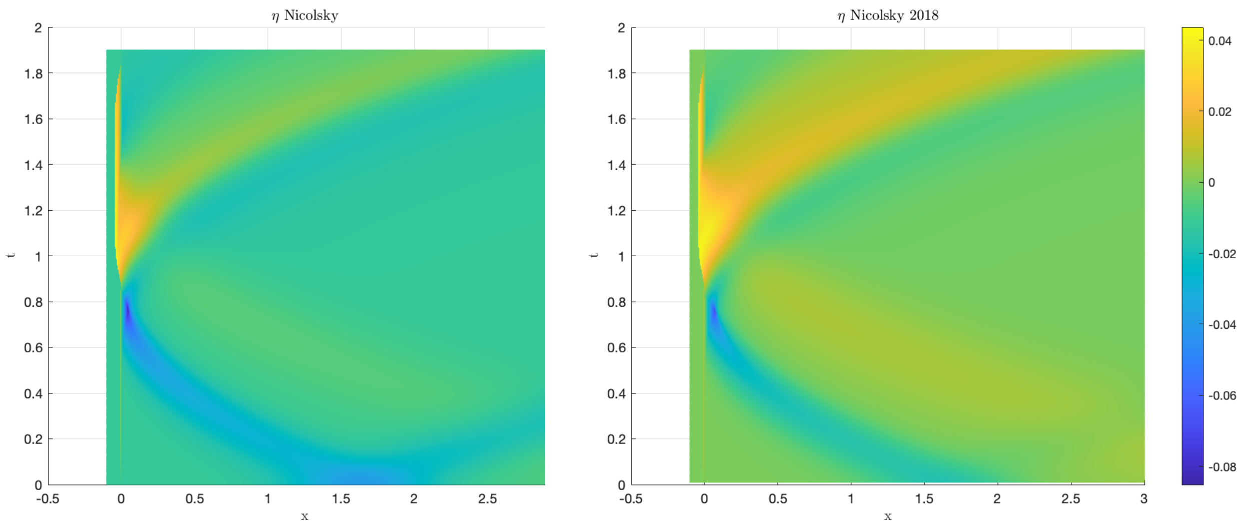

(a) Zero Velocity

(b) Non Zero Velocity

Figure 3: η Nicolsky Solution over x:[-0.1 3] and t:[0 1.9]

$$\Phi(\sigma) = -1/16 H_1 c_1 (\sigma^2 - \sigma_1^2) e^{-1/256 c_1 (\sigma^2 - \sigma_1^2)^2} + 1/16 H_2 c_2 (\sigma^2 - \sigma_2^2) e^{-1/256 c_2 (\sigma^2 - \sigma_2^2)^2}$$

Then u was computed via

$$u(\sigma, \lambda) = \int_0^\infty \xi^2 \Phi(\sigma) \left[\int_0^\infty J_1(\omega\sigma)/\sigma J_1(\omega\xi) sin(\omega\lambda) d\omega \right] d\xi$$

And η was computed via

$$\eta(\sigma, \lambda) = -1/4 \int_0^\infty \xi^2 \Phi(\sigma) \left[\int_0^\infty J_0(\omega\sigma) J_1(\omega\xi) cos(\omega\lambda) d\omega \right] d\xi - 1/2 u^2(\sigma, \lambda)$$

Then $\eta(x,t)$ and $u(x,t)$ were found via an inverse Carrier Greenspan Transform. Please see NOAA for a more complete derivation. Figure 4 depicts the solution.

3 Results

3.1 Zero Velocity (Catalina 1)

Figure 5 depicts the FVM vs. Nicolsky comparison. The L2 norm is bounded below 0.055. Notice that the solution converges at $t = 0$ but very rapidly diverges. One explanation for the difference is diffusion in the FVM.

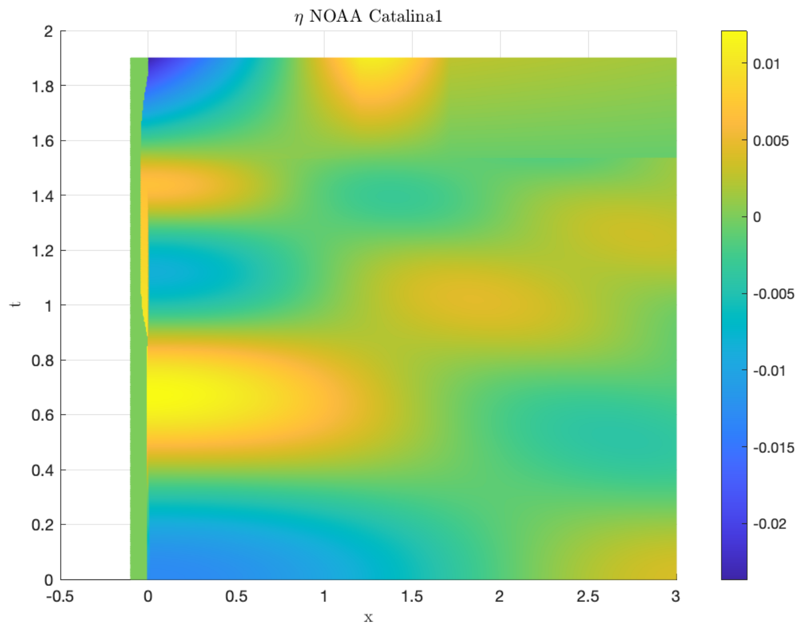

Figure 4: NOAA Catalina 1 Zero Velocity Solution

Figure 6 depicts the FVM vs. NOAA comparison. The L2 norm is bounded below 0.3, which is absolutely massive. Notice that the solution doesn't converge at $t = 0$ and the l2 norm remains high throughout the time interval.

3.2 Non-Zero Velocity

Figure 7 depicts the FVM vs. Nicolsky comparison. The L2 norm is bounded below 0.12, which is roughly double for the non-zero velocity case. Similar to the zero-velocity Nicolsky vs. FVM case, the solution converges at $t = 0$.

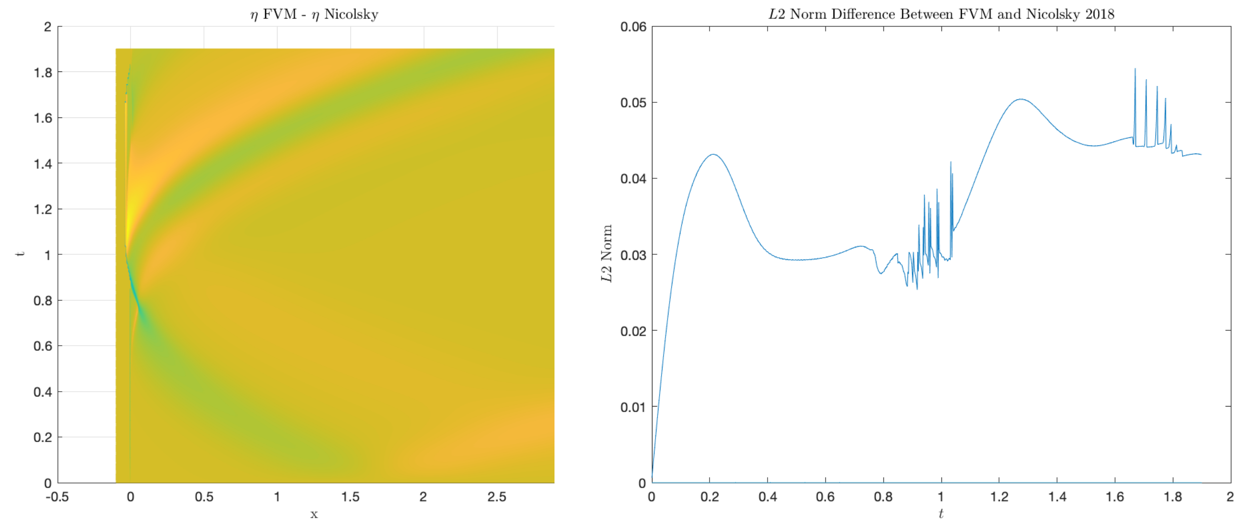

(a) Difference Between FVM and Nicolsky

(b) L2 Norm at each time

Figure 5: η FVM vs. Nicolsky Statistical Analysis

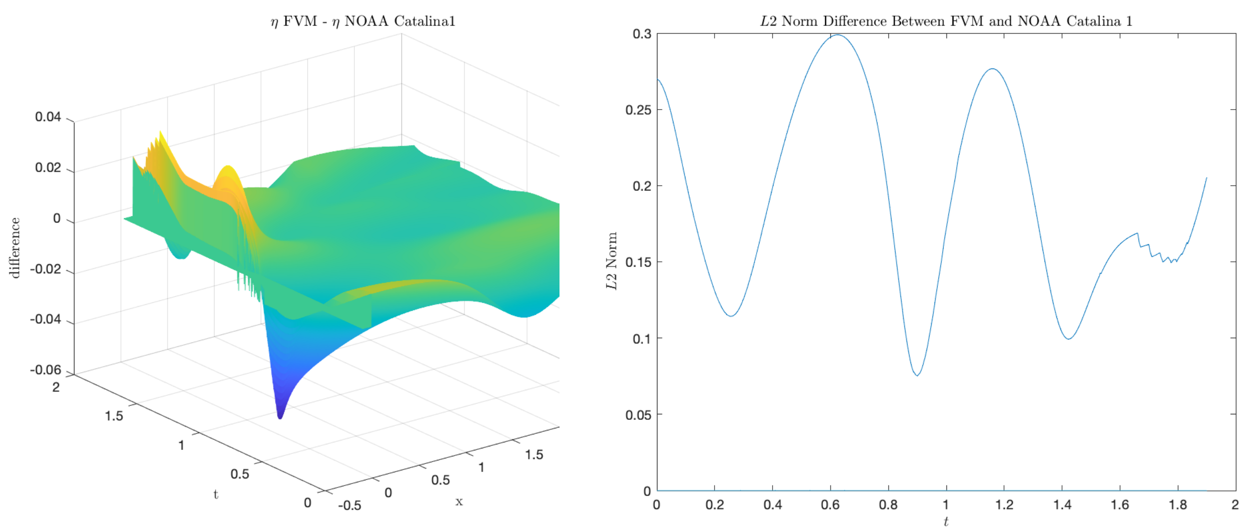

(a) Difference Between FVM and NOAA

(b) L2 Norm at each time

Figure 6: η FVM vs. NOAA Statistical Analysis

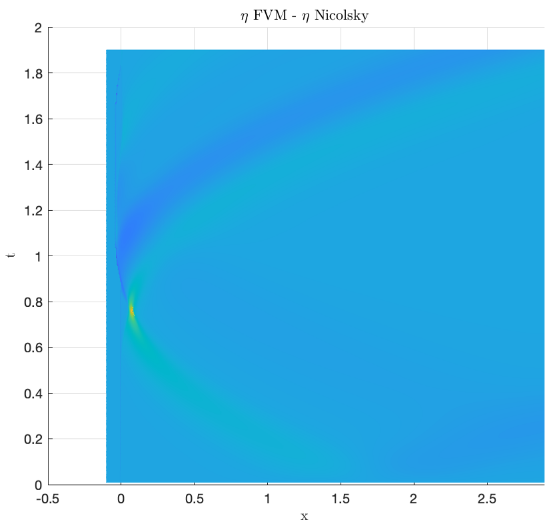

(a) Difference Between FVM and Nicolsky 2018

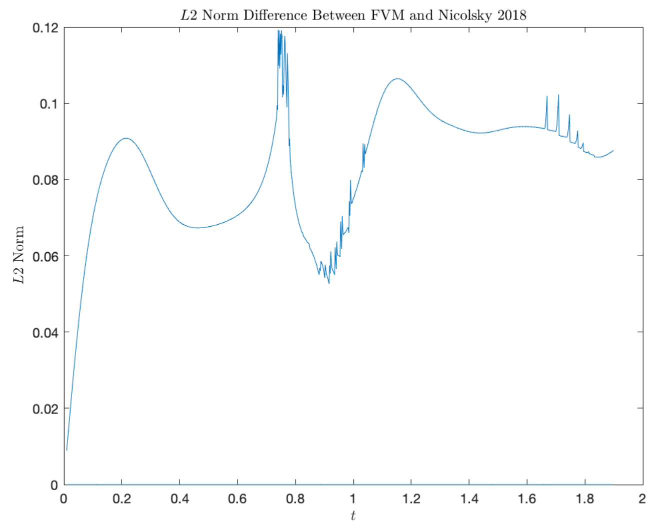

(b) L2 Norm at each time

Figure 7: η FVM vs. Nicolsky Non Zero Velocity Statistical Analysis